PERMEABILITY DAMAGE DUE TO ASPHALTENE DEPOSITION: EXPERIMENTAL AND MODELING ASPECTS

L. MINSSIEUX, L. NABZAR, G. CHAUVETEAU and D. LONGERON

Institut français du pétrole[1]

R. BENSALEM

Sonatrach[2]

ENDOMMAGEMENT D'UN MILIEU POREUX PAR DÉPÔTS D'ASPHALTÈNES : EXPÉRIENCES ET MODÉLISATION

Les propriétés d'écoulement de plusieurs bruts asphalténiques ont été étudiées à la température du réservoir d'origine dans des roches de morphologie et minéralogie différentes.

Les expériences réalisées mettent en évidence une réduction progressive de la perméabilité à l'huile au cours de l'injection, plus ou moins rapide selon les cas.

L'existence de dépôts organiques a été vérifiée par des mesures de pyrolyse « Rock-Eval » effectuées sur des sections d'échantillons prélevées en fin d'écoulement à différentes distances de la face d'entrée. Cette technique permet de quantifier le profil des dépôts.

L'interprétation des expériences de colmatage et leur simulation sont traitées en assimilant les asphaltènes dans l'huile à des particules colloïdales en suspension, susceptibles de se déposer à la surface des pores et ainsi de réduire la perméabilité du milieu poreux. Les premières simulations ont été réalisées en utilisant le modèle IFP d'endommagement particulaire « PARIS », qui a été récemment généralisé au cas de dépôt en multicouches. On observe un accord qualitatif satisfaisant avec les résultats expérimentaux.

PERMEABILITY DAMAGE DUE TO ASPHALTENE DEPOSITION: EXPERIMENTAL AND MODELING ASPECTS

The flow properties of several asphaltenic crudes were studied at reservoir temperature in rocks of different morphology and mineralogy.

The experiments performed showed a progressive reduction in permeability to oil during injection, varying in rate according to the system considered.

The existence of organic deposits was verified by "Rock-Eval" pyrolysis measurements made on sections of samples taken at the end of flow at different distances from the entry face. This technique enables the profile of the deposits to be quantified.

The interpretation of the permeability damage experiments and their simulation are treated by comparing the asphaltenes in oil to colloidal particles in suspension, capable of being deposited at the surface of the pores and thus reducing the permeability of the porous medium. The first simulations were carried out using the "PARIS" IFP particle damage model, which has recently been

(1) 1 et 4, avenue de Bois-Préau, 92852 Rueil-Malmaison Cedex - France

(2) Direction Production, 8, chemin du Réservoir, Hydra, Alger - Algérie

extended to the case of multi-layer deposition. A satisfactory qualitative agreement is observed with the experimental results.

PERDIDAS DE PERMEABILIDAD ORIGINADAS POR LOS SEDIMENTOS DE ASFALTENOS : ASPECTOS DERIVADOS DE LA EXPERIENCIA Y DE LA MODELIZACION

Se ha procedido al estudio de las propiedades de circulación de varios crudos asfalténicos a la temperatura del yacimiento de origen en rocas de morfología y mineralogía de distinta índole.

Las experimentaciones llevadas a cabo hacen resaltar una reducción progresiva de la permeabilidad al petróleo durante el transcurso de la inyección, más o menos rápida según los casos.

La existencia de sedimentos orgánicos se ha verificado mediante mediciones de pirólisis "Rock-Eval" efectuadas mediante secciones de muestras extraídas al final de la circulación fluida y a distintas distancias de la cara de entrada. Esta técnica permite cuantificar el perfil de las sedimentaciones

La interpretación de las experimentaciones de entarquinamiento (obstrucciones) y su simulación se tratan asimilando los asfaltenos en el petróleo a partículas coloidales en suspensión, susceptibles de depositarse en la superficie de los poros y, por ende, reducir la permeabilidad del medio poroso. Las primeras simulaciones se han llevado a cabo utilizando el modelo IFP de deterioro particular "PARIS", que se ha generalizado recientemente en el caso de aplicación de sedimentaciones multicapas. Se observa una concordancia cualitativa satisfactoria con los resultados experimentales.

INTRODUCTION

Production problems related to asphaltene deposition generally appear first in the field in surface facilities, especially in separators, during the oil final depressurization step [1] and [2].

Another critical point in the production chain is within production tubing in which deposits form at depths corresponding to the bubble pressure of produced oil [3] and [4]. Afterwards the asphaltene deposit zone can migrate to bottomhole and in the near wellbore formation as reservoir depletion proceeds. This is the long and well-known story of the Hassi Messaoud field [2, 3, 5].

However in some recent fields, well impairment has even started in early stages of production [6] and [7].

The in vitro flocculation phenomenon and asphaltene precipitation have been the topic of many papers. However, the effects of asphaltene flocculation in a porous medium have just recently come under investigation.

Published work deals with experiments and observations carried out in micromodels [8] and [9]. Only a few have been performed in sandpacks [10] or cores [11], generally with model fluids, i.e. a solution of crude extracted asphaltenes dissolved in toluene.

The work presented here, based on the systematic use of identified crude oils, focuses on the effects of asphaltene flocculation and precipitation upon oil flow properties in consolidated porous media. It has led to a direct laboratory evaluation of core damage due to asphalt deposition inside outcrop and reservoir-rock samples.

1 CHARACTERISTICS OF ASPHALTENIC CRUDES

Three crude oils were selected from distinct geographic origins, France, North Africa and North America. Table 1 shows the physical properties and information about the chemical composition (from SARA analysis, i.e. Saturates/Aromatics/Resins/Asphaltenes) of the stock tank oils that were used.

It can be seen that the asphaltene content covers the range from about 0.1% weight for Hassi Messaoud (HMD) crude to 6% for Weyburn crude, a Canadian oil.

TABLE 1

Characteristics of stock tank oils considered

Field	Reservoir temperature (°C)	SARA analysis				Res./Asph. ratio	Viscosity (cP 20°)	°API
		Sat.	Ar.	Resins	Asph.			
Weyburn	50	40.1	46.1	8.5	5.3	1.6	13	29
Lagrave	80	65.7	22.8	7.5	4	1.9	7.7	43
Hassi Messaoud	119	70.5	25.5	3.3	0.15	22	1.5 (80°)	43
Boscan (reference)	81	15	37	34	14	2.4		10

Boscan crude features have been added in this table for the purpose of comparison as this well-known *trouble-free* asphaltenic oil is often referred to in published asphaltene studies.

The resin to asphaltene ratio in crude most polar fractions is also given as it is often used as an indication of asphaltene solubility in crude oil. Resins are thought to be good dispersing agents for asphaltenes. Unfortunately, this ratio seems to be useless in the case of low asphaltene oil contents, such as those found in the Hassi Messaoud crude, a well-known example that illustrates long term production problems due to asphaltene deposition.

2 EXTRACTION AND ANALYSIS OF SOLID ASPHALTENES

Asphaltenes have been extracted from each crude oil using the French T60-115 method with *n*-heptane precipitation. Specific analytical data for isolated asphaltenes are given in Table 2, including molecular weight (MW) from vapor pressure osmometry (VPO) and elemental analysis.

Isolated asphaltenes were also pyrolyzed in a Rock-Eval apparatus as described in Section 5. An example of the pyrogram obtained with HMD asphaltenes is discussed in Section 8.

Asphaltenes were also characterized by means of the TG-FTIR technique combining pyrolysis and thermogravimetry with periodic infrared spectrum sampling. An example of results obtained with the asphaltenes from an Alaskan crude oil similar to Weyburn asphaltenes is given in Figure 1, which traces the different functional groups cracked during the pyrolysis process (involving the N, C, O, S heteroatoms usually present in most asphaltene fractions). The series of spectra was found to be identical for the three asphaltenes that were analyzed, which means that their common functional groups were released within the same temperature range. This indicates that, although asphaltene fractions can be complex molecular species mixtures, they convey, as a whole, an obvious chemical similarity, irrespective of crude geographic origin.

TABLE 2

Crude/asphaltene characteristics

Crude origin (°API)	% Asphaltene (weight)	Average MW (VPO/toluene)	Asphaltene analysis			T_{max} (°C) pyrolysis
			Atomic H/C	Atomic O/C	% weight S	
Weyburn 29	5.3	6000	1.00	0.025		416
Lagrave 43	4	7000 to 8700	1.00	0.010	3.80	416
Hassi Messaoud 45	0.15	1120 “well scales”	0.88	0.034	0.80	420
Boscan (10°) (reference)	14	8000	1.14	0.039	6.70	406

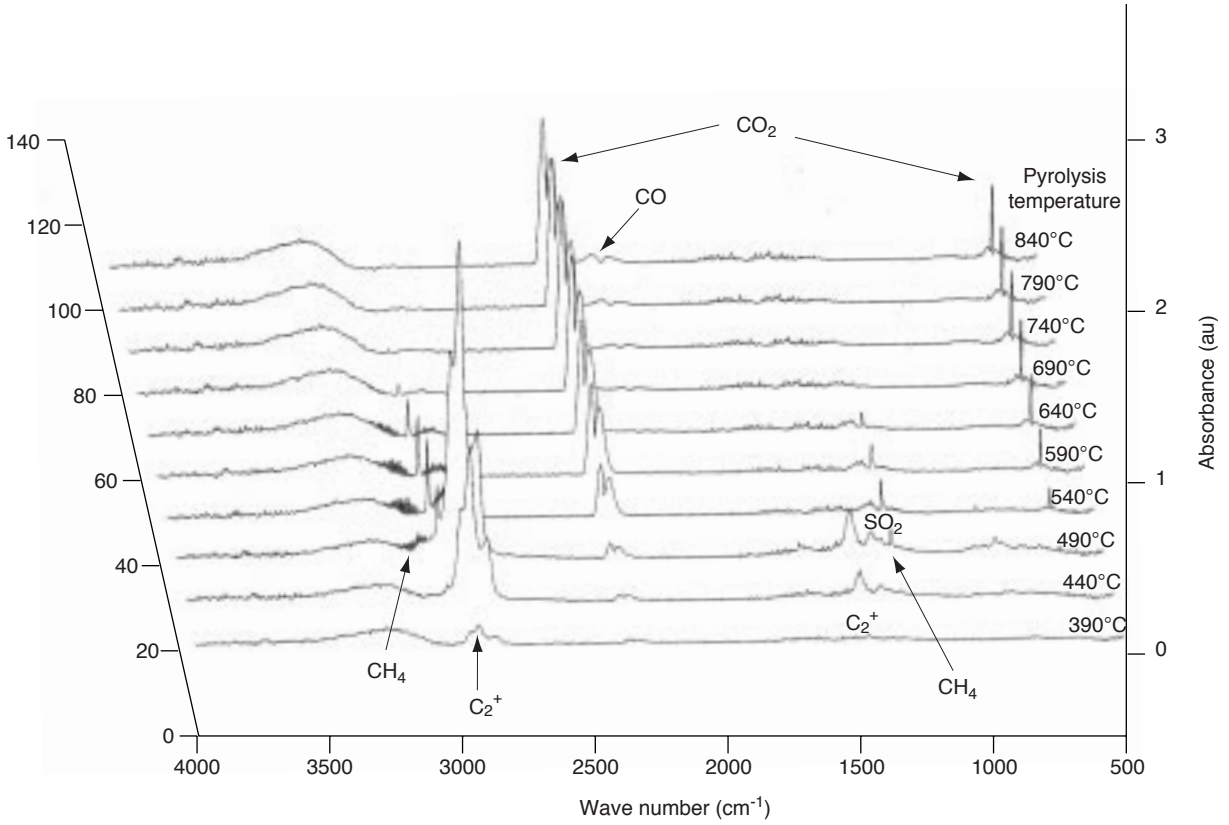

Figure 1

Analysis of Weyburn asphaltenes by means of the TG-FTIR technique.

Perhaps this can be explained by a similar geochemical origin for the crude oils that have been studied.

3 POROUS MEDIA SELECTION

Porous media selected for oilflood tests were the following:

– Outcrop consolidated samples: Fontainebleau sandstone, a so-called model porous medium, made of pure silica (no clay present) and showing regular grain size and morphology.

– Vosges clayey sandstones containing illite and tight Pfalz sandstones containing kaolinite.

Using the Purcell method, the predominant pore radii were estimated to be in the range of 5 to 10 µm for Fontainebleau sandstone, 2 to 10 µm for Vosges sandstone and 0.3 to 3 µm for Pfalz sandstone.

– Hassi Messaoud (HMD) core samples were included as an example of reservoir rock and several corefloods were carried out with Hassi Messaoud crude oil. This reservoir rock contains kaolinite as the main clay mineral.

The core dimensions used, diameter 2.3 cm, length 5 to 7 cm, were chosen so as to enable injection of large fluid volumes within reasonable periods of time.

Cleaning of core samples was performed by means of soxhlet extraction with toluene.

Water permeability of the cores used was low (2 mD) to moderate (100 mD) as shown in Table 3.

4 PROCEDURE FOR CORE PLUGGING EVALUATION

The following testing conditions were defined and systematically used here as a standard method for measuring core damage at reservoir temperatures, resulting from asphaltenic crude oil flow in porous media. It includes the following steps:

– Saturate core with brine (KCl 30 g/l) and measure water permeability.

– Flood with cyclohexane to connate water saturation and determine oil relative permeability.

  Connate water saturation was deemed a realistic condition considering the fact that the presence of water is known to modify somewhat [16] the adsorption isotherms of asphaltenes onto minerals representative of reservoir rock.
– Flood with the crude oil at constant flow rate, at least 100 pore volume throughput, with continuous recording of differential pressure.
– Flood with cyclohexane to determine the final reference hydrocarbon permeability after asphaltenic oil flow, in order to evaluate the extent of core damage.

  The use of cyclohexane as a reference oil was chosen because, at the end of crude injection, it is necessary to displace miscibly the crude in place by a fluid that neither causes any extra deposition nor dissolves the asphaltene deposits left after crude oil flow. As shown by the comparison of saturated hydrocarbon precipitation properties in work by Mitchell and Speight [12], cyclohexane fulfills this double requirement.
– The final step in the test consists of cutting the core into sections and crushing them for Rock-Eval analysis as detailed below.

5 ROCK-EVAL ANALYSIS OF ORGANIC DEPOSITS IN CORE SAMPLES

In order to describe the plugging mechanisms in a porous medium, a method is needed to detect and measure the amount of deposits retained within the core after the oil flow test.

In this work we have adapted for that purpose the Rock-Eval technique [13] commonly used by geochemists for source rock analysis.

The apparatus permits measurement of the quantity of pyrolyzed hydrocarbons during a preset heating program designed for the heavy oil fractions of interest here. After an initial period of 15 minutes at 180°C, the temperature is increased by 10°/min until a final temperature of 650°C is reached.

Three distinct surfaces generally appear as shown in Figure 2. They correspond to the different hydrocarbon

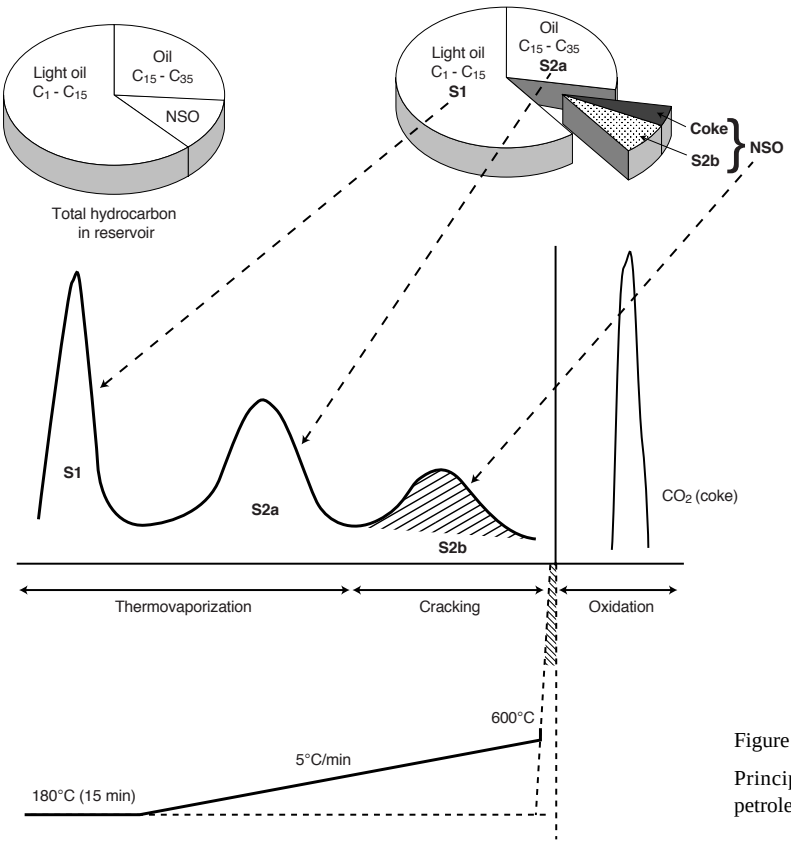

Figure 2

Principle and schematic pyrogram for pyrolysed petroleum residues.

fractions released during pyrolysis. The last one, the "S2b" peak, corresponds to the pyrolysis of the heaviest compounds of concern in this work, i.e. asphaltenes possibly mixed with some resins. Related amounts of organic material, expressed in milligrams per gram of rock, are calculated from peak surface determinations.

Stock tank oils, their extracted asphaltenes and resin fractions separated via HPLC, were pyrolyzed in the same apparatus to get typical reference pyrograms. We discuss the results obtained in the case of HMD crude oil in Section 8.

6 CORE FLOOD RESULTS AND DISCUSSION

The operating conditions for each test as well as the stock tank oil and porous medium used, are shown in Table 3. Core tests were performed at 50°C or 80°C, with a back pressure of 10 bar.

The table also contains the petrophysical data for core samples.

Plugging effects obtained during each run, after at least 50 PV (number of pore volumes injected into the core sample), are compared in Table 4.

As described above, core damage, expressed as K/K_o, has been evaluated at the end of test in terms of reduced cyclohexane initial (S_{wi}) permeability.

The table also gives the Rock-Eval average amount of organic deposits left in situ as well as a qualitative description of final deposit profiles found along each core considered. They exhibit two typical distributions: either nearly uniform or clearly decreasing from core inlet.

7 CORE PLUGGING PROCESS

For the whole series of tests, plugging is generally observed only after a sufficient volume of oil has passed through the core, at least 20 to 50 PV. This is especially the case for crude with a low asphaltene content such as HMD crude oil (see runs GF 12 and HMD 26 in Table 4), or in a porous medium which does not contain any adsorbing minerals.

TABLE 3

Conditions for core floods

Test ref.	Type of rock	T (°C)	Crude used	Petrophysical data		Flow rate (cm^3/hour)
				ø %	K_H (mD)	
GF 1	Fontainebleau sandstone	50	Weyburn	13.1	107	50 (64 PV) 80 (94 PV)
GF 2	id.	id.	id.	13.6	87	10
GF 3	id.	id.	id.	13.7	77.4	10 (82 PV) 20 (221 PV) 50 (120 PV) 80 (184 PV)
GF 12	id.	80	H. Messaoud	8	6	10
GVM 5	Vosges sandstone	50	Weyburn	24.7	29	10
GVM 10	id.	50	Weyburn	24.3	12.2	10 (48 PV) 5 (40 PV)
GVM 13	id.	80	Lagrave	26	73	10
GVR 8	id.	50	Weyburn	22.6	15.2	10
GVR 11	id.	80	Lagrave			
GP 9	Pfalz sandstone	80	H. Messaoud	22.6	1.1	10 (40 PV) 5 (25 PV)
GP 14	id.	id.	id.	23	2	5
HMD 11	Res. rock from HMD	id.	id.			
HMD 26	id.	id.	id.	7.1	0.67	8

TABLE 4

Coreflood tests

Test ref.	Crude used	Average amount of deposits (mg/g rock)	Deposition profile inlet → outlet	K reduction (%) after 50 PV	Observations
GF 1	Weyburn			20	Reference model of a porous medium (pure silica)
GF 2	W.	0.30	Uniform	42.5	
GF 3	W.	0.21	Uniform	58.5	
GF 12	HMD	0.34	Decreasing	0 47 after 150 PV	
GVM 5	W.	1.0	Decreasing	88	Vosges clayey sandstone (illite)
GVM 10	W.	0.48	Decreasing	89	
GVM 13	Lagrave	–	–	< 19	Additive in flowing crude (750 ppm)
GVR 8	W.	0.11	Decreasing	87	Vosges sandstone II
GVR 11	Lagrave	< 0.10	Near core inlet accumulation	–	Final K_H difficult to measure
GP 9	HMD	0.33	Decreasing	60	Pfalz sandstone (kaolinite)
GP 14	HMD	No plugging		–	Crude injected with additive
HMD 11 + HMD 26	HMD	0.58 (“Resins”) 0.41 (“Resins”)	Uniform Uniform	 6 (50 after 700 PV)	Composite core made up from two Hassi Messaoud reservoir rock samples

The core damage progresses according to a more or less slow process as illustrated in Figures 3 to 7, which show the evolution of oil permeability as a function of pore volumes of crude oil injected:

– K_{oil} decreases steadily and linearly (Figs 3, 7), or
– K_{oil} decreases more drastically, then approaches an asymptote (Figs 4, 5).

It should be noted here that in the whole series of oil corefloods, external caking on the core inlet was never observed. This means that asphaltenes contained in injected crude oils could penetrate into the pore framework without external filtration.

The most noticeable plugging was observed in clayey Vosges sandstone containing illite (Fig. 5) and in tight Pfalz sandstone (Fig. 6) containing kaolinite.

In these types of rocks, permeability reduction starts with an important adsorption of asphaltenes onto high specific area clays, then is followed by hydrodynamic retention of asphaltene aggregates at pore throats.

As expected, the pore morphology of the rock sample is also involved in the plugging process. In lower permeability samples, core damage is more extensive (see runs GF 1, GF 2 and GF 3 in Tables 3 and 4).

It may be that the plugging effects observed with stock tank oils at reservoir temperature should a fortiori exist during depletion of live oils as it is known that asphaltenes exhibit *minimal solubility in crude oil near its bubble point* [14] and that solubility increases again at lower pressure.

8 COMPOSITION OF ORGANIC DEPOSITS IN CORE SAMPLES

Rock-Eval analysis provides some qualitative information about the chemical nature of *in situ* organic deposits. Thus, core sample pyrolysis results at the end of test, in the temperature range 200°C to 500°C, indicate a high concentration of asphaltenes in organic deposits (Fig. 8) obtained at the end of run GP 9 in which the core deposit pyrogram is compared to those given by the injected crude oil and extracted asphaltenes.

This is what was observed in most runs. Interestingly, in the run with HMD reservoir-rock and associated crude oil containing much more resin than asphaltene (Table 1), Rock-Eval analysis clearly demonstrates that the resin fraction is predominant in deposits, since pyrograms exhibit a clear peak

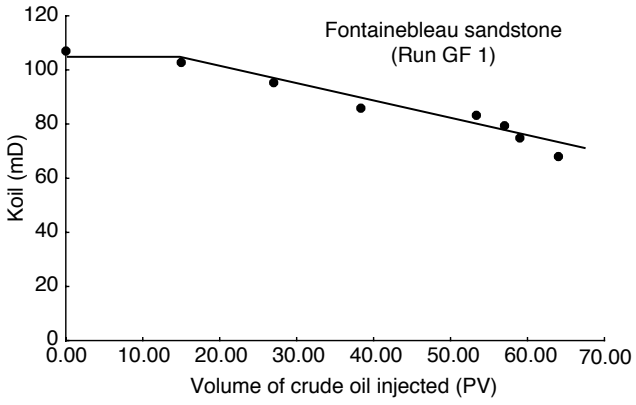

Figure 3

Oil permeability reduction in a model-porous medium.

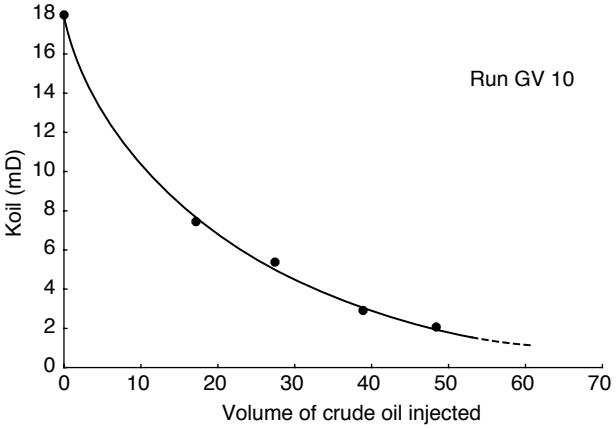

Figure 4

Oil permeability reduction in Vosges sandstone.

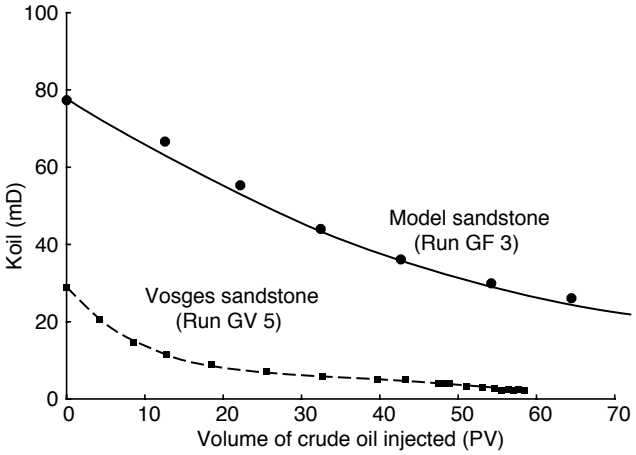

Figure 5

Oil permeability reductions compared in the presence and absence of clay minerals.

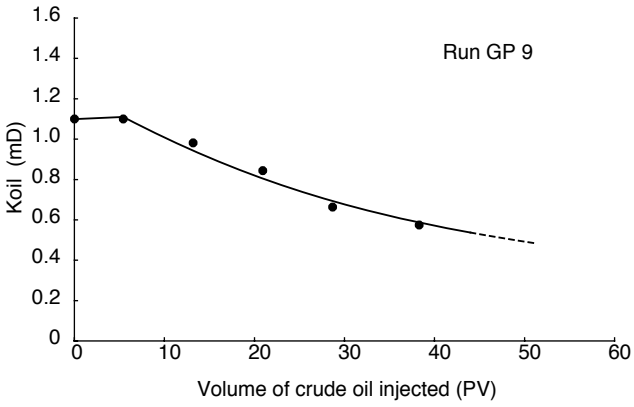

Figure 6

Oil permeability reduction in a tight Pfalz sandstone.

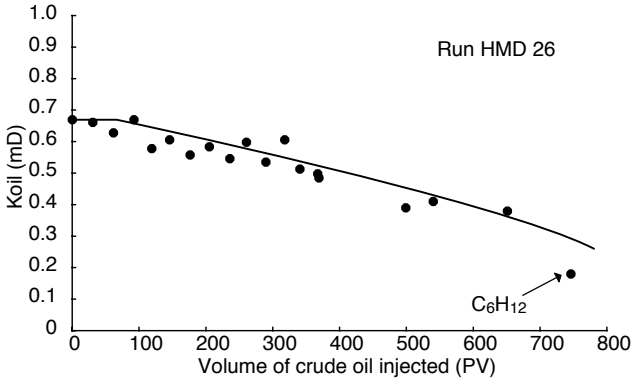

Figure 7

Oil permeability reduction in a Hassi Messaoud reservoir core sample.

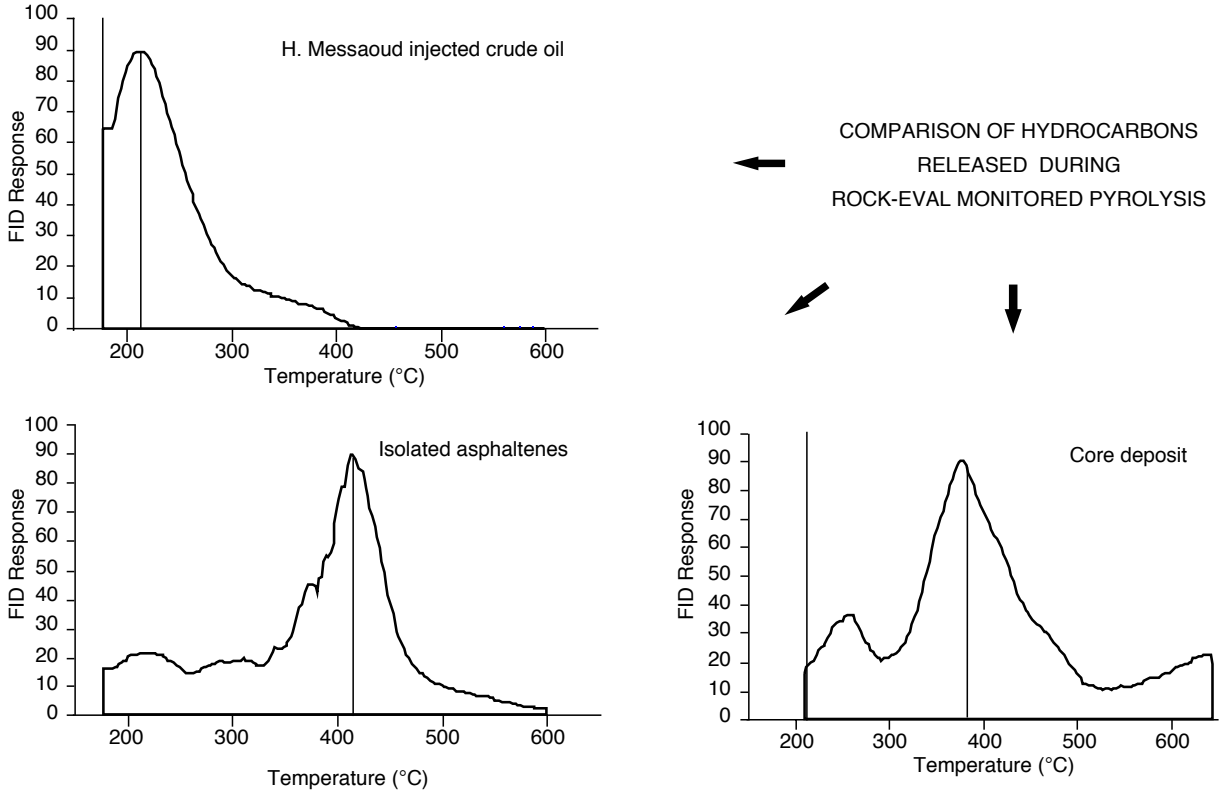

Figure 8

Rock-Eval pyrograms for organic deposits in a Pfalz sandstone core sample.

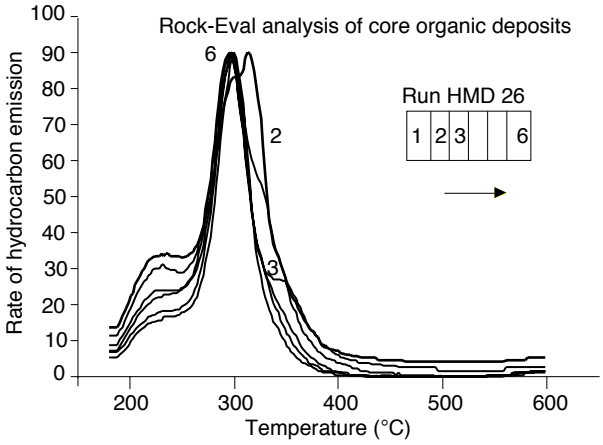

Figure 9

Deposition profile of heavy fraction deposits in a Hassi Messaoud reservoir core sample.

at 300° (Fig. 9), i.e. at the thermo-vaporization temperature of the crude oil resin fraction. This observation presumably results from the specific chemical composition of HMD crude oil (i.e. its high resin to asphaltene ratio) combined with the nature of the minerals present in the home reservoir-rock.

9 MECHANISMS AND INTERPRETATION OF CORE PLUGGING EXPERIMENTS

Before the plugging process develops, an initial step presumably involves the fast adsorption of polar and high molecular weight asphaltenes onto free active sites on the rock surface. This is especially the case for clay minerals such as kaolinite, as suggested by published isotherms [14] and [15]. Then, thicker molecular structures, i.e. multilayers, presumably form as indicated by the absence of a plateau in the adsorption isotherms of Ceuta, Furrial and Boscan asphaltenes onto quartz surfaces, published by S. Acevedo [16]. It is also relevant to mention here the results of continuous adsorption experiments obtained by Piro [10] with toluene asphaltene solutions flowing through a dolomite sand pack.

In the third step, due to the dynamic aggregation phenomenon among asphaltene molecules suspended in the oil, large aggregates can form within pores. As these processes occur, a fraction of the flowing asphaltenes can be trapped at pore throats, progressively extending the damaged sections of the porous medium.

This scenario is consistent with published photographs of asphaltene aggregates seen in micromodels [8] and [9] and the core deposit profiles obtained using the Rock-Eval technique (Table 4).

Considering all the experimental results, it should be emphasized that the core plugging effects observed with several asphaltenic crudes exhibit very similar trends, both in reducing permeability and accumulating *in situ* deposits with core damage results from the migration of fine-grained solid particles accompanying brine flow through the porous medium [18, 19, 20].

These similarities in the plugging mechanisms in a porous medium caused by solid particles led us to apply related models to the interpretation of experiments carried out with colloidal asphaltene particles present in crude oils.

10 MODELING ASPECTS

Most published studies related to asphaltenes have investigated chemical structure and techniques to remedy formation damage using injected additives to inhibit asphaltene adsorption and deposition. Modeling asphaltene retention and its effects on permeability in order to predict productivity decline has not been based on a consistent physics until now, due to the lack of a sufficiently good understanding of the asphaltene/crude oil system. Even though this system is generally recognized as colloidal, little is known about the physical and chemical properties of asphaltene particles or their particle size and distribution. The goal of this section is to see whether a colloidal approach can help providing insight into the mechanisms involved in asphaltene deposition and related permeability impairment.

Considering the asphaltene/crude oil system as a colloidal suspension, model predictions using the PARticle Injection Simulator (PARIS model) developed for solid colloidal particles [21] and [22] have been compared with the results of some of the previous corefloods carried out under controlled conditions.

10.1 Main Features and Basic Equations of the Model

10.1.1 Representation of a Porous Medium

The porous medium is macroscopically represented by a series of slices or unit bed elements (UBE). Each UBE is presumed to consist of a collection of unit cells or collectors (Fig. 10). The choice of the unit cell and its characteristic dimensions are based on the GPT model [23].

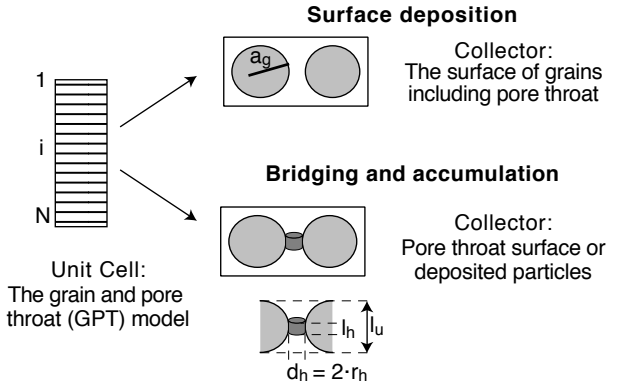

Figure 10

Representation of a porous medium.

The three geometrical characteristics of the GPT model, namely the unit cell size l_u, the hydrodynamic pore throat length l_h and diameter d_h, are defined by:

$$l_u = \left[\pi / 6(1-\phi)\right]^{1/3} . d_g$$

$$d_h = 2 \cdot C \cdot \sqrt{8K_o / \phi} \qquad l_h = \frac{\pi}{128} \cdot \frac{d_h^4}{l_u . K_o}$$

where ϕ is the porosity, K_o the initial permeability, d_g the grain diameter and C a characteristic constant of the porous medium ($C = 1.15$ for granular packs, $C \simeq 0.5$ to 5 for consolidated sandstone).

10.1.2 Governing Equations for Multilayer Deposition

Our modeling efforts were geared toward a first evaluation of how well the PARIS model accounts for the permeability impairment due to surface deposition

during asphaltenic crude oil flow through model porous media. Moreover, there is clear experimental evidence that asphaltene retention during core flow experiments takes place as multilayer deposits onto mineral surfaces [10]. Thus, a "multilayer version" of the PARIS model is developed and used here.

Local Deposition Flux

In the convection-diffusion regime, the general expression for the local deposition flux is given by [22] and [24]:

$$j_l^i(\theta) = \mathrm{P}_d \cdot K_l(\theta) C_f^i \qquad (1)$$

where:

- C_f^i is the particle concentration in the flowing liquid;
- K_l is the transfer coefficient which is a local function of the flow rate and of the azimuthal position angle θ measured from the forward stagnation point. Indeed, in the PARIS model, the deposition rate is considered to be non-uniform around the collecting grain, being higher near the forward stagnation point and decreasing as θ increases;
- P_d is the deposition probability.

The deposition step is a complex process controlled by the physicochemical and hydrodynamic conditions prevailing in the vicinity of the collector surface. This is generally encompassed in a macroscopic parameter, η, called the single collector capture efficiency. It is defined as the fraction of the particles captured inside a flow tube parallel to the mean flow direction and with a cross section equal to the projected area of the collector (A_c). The capture efficiency is related to the commonly used filter coefficient λ through:

$$\eta = \frac{\lambda}{A_c N} \qquad (2)$$

where N stands for the number of collectors per unit volume.

Using the capture efficiency parameter, the deposition probability may be expressed as:

$$P_d = \frac{\eta}{\eta_o} B(\theta) = \alpha B(\theta) \qquad (3)$$

where:

- $B(\theta)$ is the local dynamic blocking function (DBF) which takes into account the effect of previously deposited particles on the deposition rate.
- η and η_o are respectively the capture efficiency in the presence and in the absence of an energy barrier between particle and collector.

If ΔG is the activation energy for particle deposition in the presence of an energy barrier between particle and collector, we have:

$$\alpha = \frac{\eta}{\eta_o} = \exp\left(-\frac{\Delta G}{kT}\right) \qquad (4)$$

An analytical expression giving the relative capture efficiency, α, may be found in earlier published work [22] and [24].

When using a dynamic blocking function equal to the local free surface fraction (Langmuir type deposition), the deposition probability for multilayer deposition may be related to the free surface fraction, $F_o^i(\theta)$, and to the relative capture efficiencies α^b and α^c, respectively corresponding to the bare (monolayer formation) and covered (multilayer formation) surface fraction. Thus, P_d may be expressed as:

$$P_d = \left[\alpha^c + \left(\alpha^b - \alpha^c\right) F_o^i(\theta)\right] \qquad (5)$$

Note that, for a more rigorous treatment, the relative capture efficiency α^c should be linked to the local shear rate. Thus, it should not be kept constant, but allowed to decrease as multilayer formation progresses. Indeed, in contrast to monolayer deposition, multilayer formation leads to a continuous increase in the local shear rate as a consequence of pore throat size reduction. This is expected to prevent asphaltene deposition or to detach the previously deposited particles (high shear rate) resulting in a progressive decrease of the multilayer deposition rate.

Local Deposition Density

Following Priveman *et al.* [25], the rate of monolayer formation can be written as:

$$-\frac{\partial F_o^i(\theta)}{\partial t} = \alpha^b \beta_c F_o^i(\theta) K_l^i(\theta) \cdot C_f^i \qquad (6)$$

The deposition density is then obtained from Equations (1), (4) and (5) as:

$$\beta_c \Gamma_l^i(\theta) = \left(1 - \frac{\alpha^c}{\alpha^b}\right)\left(1 - F_o^i(\theta)\right) - \frac{\alpha^c}{\alpha^b} \ln\left[F_o^i(\theta)\right] \qquad (7)$$

where β_c is the reciprocal maximum deposition density corresponding to monolayer saturation.

Permeability Reduction

Permeability reduction is usually evaluated in two different ways:

– Using the bundle capillary model and Poiseuille's law. The deposition is then assumed to take place in a smooth layer which gradually reduces the capillary radius.

– Using the Happel "sphere-in-cell" model and the empirical Kozeny-Carman equation to convert the total specific deposit, through a decrease in porosity, into a permeability reduction.

However, both methods fail to predict correctly the permeability reduction versus pore volumes injected mainly for two reasons:

• the pore structure is ignored or is unrealistic;

• the pore structure is actually such that the effect of retained particles on permeability *depends drastically on their location within the porous medium.*

In the PARIS model, the local permeability is linked *only to the retention occurring in the pore throats.* Therefore, in the case of multilayer surface deposition, the permeability reduction is a consequence of gradual pore throat size reduction by asphaltene deposition. Using the GPT model [23] and Poiseuille's law, the following expression for the local permeability reduction may be derived:

$$R_k^i = k/k_O = \left[1 - \frac{\delta_h}{r_p}\right]^4 \qquad (8)$$

where r_p is the initial pore throat radius and δ_h the hydrodynamic thickness of the deposit on the pore throat surface. After a few mathematical manipulations, Equation (8) can be expressed as:

$$R_k^i = \left[1 - N_{pt}\frac{v_p}{4\pi a_g r_p^2}\right]^2 \qquad (9)$$

v_p being the particle volume, N_{pt} the total number of particles deposited on the pore throat surface and a_g the grain (collector) radius. Equations (6-9) together with the material balance equation are the governing equations of the PARIS model multilayer version.

10.2 Results and Discussion

For colloidal suspensions of known particle size, two parameters are used in the model and must be determined experimentally through specifically designed laboratory tests:

– The bare collector capture efficiency α^b which is related to the particle/rock surface collision efficiency α^b_{pc};

– The covered collector capture efficiency α^c which is related to the particle/particle collision efficiency α^b_{pc}.

For a given system, these parameters are thought to account for all the factors controlling the deposition process. However, in the case of asphaltene particles suspended in crude oil, the actual mean aggregate size is generally unknown. Thus, the mean particle size is first used as a third parameter in a series of simulation runs whose goal is to study the effect of model parameters and to obtain a rough estimate of the mean particle size of asphaltene aggregates.

After a sufficient number of pore volumes have been injected (PVI), all preliminary simulation results show the following:

– A uniform deposition profile is established along the core;

– The permeability reduction tends to level-off to a non-zero value;

– The reduced outlet particle concentration reaches a quasi-unit value. However, saturation conditions are not attained even after 80 pore volumes have been injected (PVI).

Similar results have been reported by G. Piro *et al.* [10], who carried out core flow experiments with asphaltene (Northern Italy crude oil/*n*-heptane) in solution with toluene and dolomite sand-packs. These authors also reported that the difference between outlet and inlet concentration decreases as flow rate increases. This is in line with our previous results [22, 24, 26] obtained with solid colloidal particles and supports the colloidal approach adopted here.

In the present case, experiments GF 2 and GF 3 corresponding to Weyburn crude oil injection through Fontainebleau sandstone, led to the same long term behavior (Table 3, Fig. 5). Thus, they were selected for model validation. The GPT characteristic dimensions of the corresponding cores are shown in Table 5, while experimental conditions may be found in Tables 1 and 3.

TABLE 5

GPT unit cell characteristics

	l_u (μm)	l_h (μm)	d_h (μm)	d_g (μm)
Core GF 2	126	25.1	10.3	150
Core GF 3	127	24.9	10.0	150

10.2.1 Parameter Estimations

The effect of particle size on permeability reduction was studied for different values of α^b and α^c. Typical simulation results are shown in Figure 11. For a given set of capture efficiencies, we observe that the smaller the particle size, the more severe is the formation damage. When qualitatively comparing simulation and experimental results, we find that the mean particle size should be comprised between 5 and 20 nm. Thus, instead of a trivial parameter adjustment procedure, we decided, somewhat arbitrarily, to choose a mean particle size of 10 nm for the asphaltene aggregates. Asphaltenes in crude oil are generally viewed as aggregates with an approximate density of 1.2 g/cm^3 and a radius of gyration ranging from 3 to 7 nm, depending on the chemical composition of the crude and particularly on its asphaltene peptizing resin content [27] and [11].

On the other hand, for a given particle size, simulation results showed clearly that (Fig. 12):

– The initial slope of the permeability reduction versus pore volume injected is determined by α^b independently of α^c;

– The final value of the permeability reduction is determined by α^c independently of α^b.

Thus, these two limiting behaviors may be used to determine the two capture efficiency parameters from a single experimental test. According to this procedure, α^b and α^c were determined using data from experiment GF 3. They were found to be equal respectively to 0.14 and 0.76. These high values indicate that the asphaltene suspensions in the Weyburn crude are composed of weakly repulsive (activation energy ~ 0.3 kT) and adsorbing aggregates (activation energy ~ 2 kT). Thus, the asphaltene deposition process is expected to be mainly diffusion limited.

10.2.2 Model and Experiments

The selected experiments, GF 2 and GF 3, were carried out, injecting the Weyburn crude in two Fontainebleau core samples with slightly different petrophysical properties (Tables 3 and 5).

Using a 10 nm average particle size and the estimated capture efficiencies from the initial and long time asymptotic behavior, the predicted permeability reduction versus pore volumes injected is in excellent agreement with experimental results from run GF 3 (Fig. 13). However, when the same parameters are used with GF 2 experimental data, a very similar permeability reduction profile is obtained (Fig. 14, run 1). This prediction is in apparent contradiction with the experiment. Indeed, experimental results show a significant difference of permeability reduction

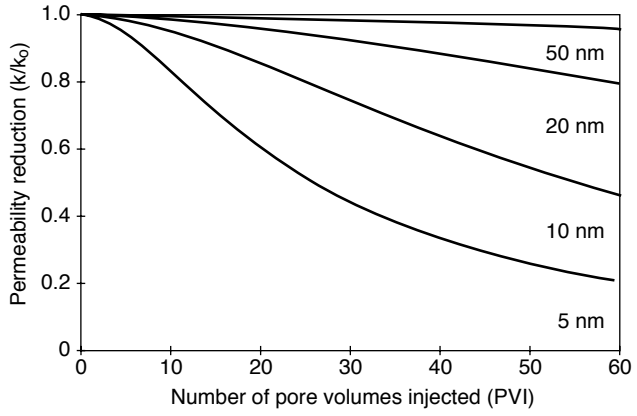

Figure 11

Simulation of core damage in run GF 3: effect of average particle size of asphaltene aggregates ($\alpha^c = \alpha^b = 0.5$).

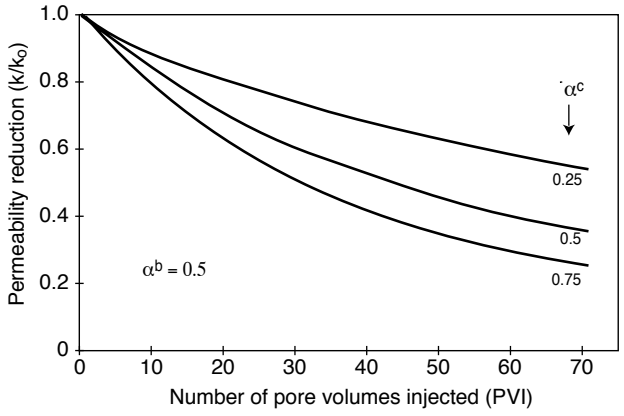

Figure 12

Simulation of core damage in run GF 3: effect of asphaltene/asphaltene interaction energy (multilayer formation) for given values of asphaltene/rock interaction (α^b) and particle size (10 nm).

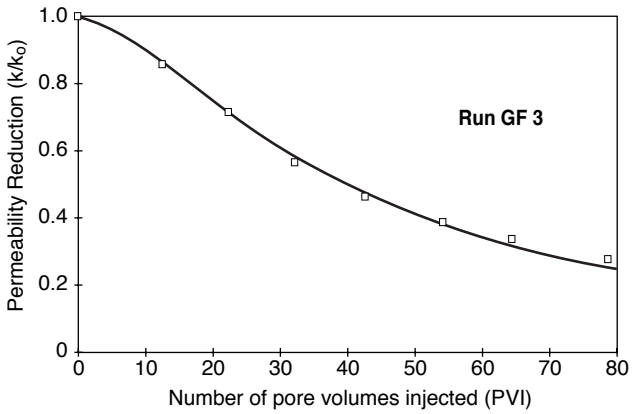

Figure 13

Experimental data in run GF 3 (symbols) vs PARIS model prediction (full line) with: $\alpha^b = 0.14$, $\alpha^c = 0.76$, $\alpha^p = 10$ nm.

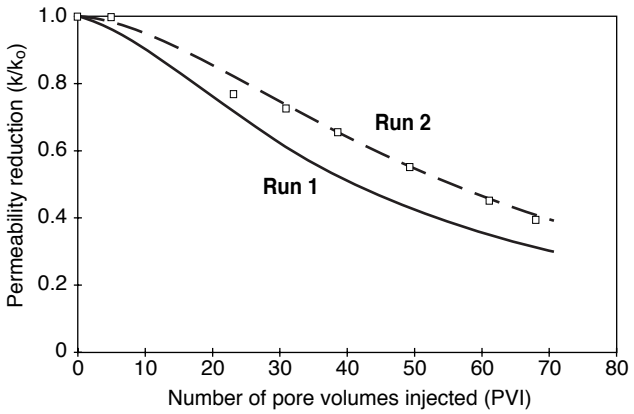

Figure 14

Simulation of run GF 2 (symbols) with the PARIS model (full lines): run 1: prediction with the same input parameters for GF 2 and GF 3 samples; run 2: prediction using a new estimated asphaltene/rock interaction energy ($\alpha^b = 0.057$).

profiles between GF 2 and GF 3, in spite of the similarity in petrophysical properties. Then, by more closely inspecting the permeability reduction versus PVI curves, we observed that the difference is significant and originates from a difference between the initial slopes. According to our theoretical development, we conclude that the difference between the two experimental results may originate from a difference in rock surface properties of the two Fontainebleau sandstones (electrochemical, residual water saturation, etc.). Thus, a new value of the capture efficiency α^b was estimated to be 0.057, corresponding to an activation energy of 3 kT. When this value is used, good agreement between model prediction and experimental results is achieved for the run GF 2 as well (Fig. 14, run 2).

CONCLUSIONS

This work provides evidence that asphaltenic oil flow through core samples can cause reservoir rock oil permeability to be reduced. Sufficient oil throughput is necessary in the laboratory in order to reproduce and observe the plugging process resulting from in situ asphalt material deposition.

Existence of in situ asphaltene deposits has been checked by Rock-Eval pyrolysis analyses. This technique also provided final deposition profiles within the tested core samples.

Analysis of plugging experiments carried out with asphaltenic crudes in several types of porous media shows clear similarities with the permeability reduction caused by the migration of fine particles accompanying brine injection.

On the basis of such observations, the PARIS simulator, designed for solid particle migration in a porous medium, was used in order to help the interpretation of plugging effects related to asphaltene deposition. Thus, for a given estimation of asphaltene particle size, it is shown that the permeability reduction during asphaltenic crude flow in a model porous medium can be satisfactorily matched using this model.

ACKNOWLEDGMENTS

We wish to express here our appreciation to B. Prempain and J. Grabias who performed the coreflood experiments, as well as to the *Sonatrach Company* which kindly supplied the Hassi Messaoud crude oil and reservoir core samples. It is also a pleasure to acknowledge the contributions of F. Marquis for all Rock-Eval analyses and J. Bonnard for collecting TG-FTIR data.

REFERENCES

1 Garland E. (1989) The asphaltic properties of an apparently ordinary crude oil. May lead to re-thinking of field exploitation. *SPE* 19731, Fall Meeting, San Antonio, October 8-11.

2 Leontaritis K.J., Amaefule J.O. and Chariles R.E. (1994) A systematic approach for the prevention and treatment of

formation damage caused by asphaltene deposition. *SPE* Prod. Fac., Aug. 1994, 157-164.

3 Briant J. (1963) Sur quelques facteurs influençant la formation de certains dépôts (paraffines, asphaltènes) dans les installations de production. *Revue de l'Institut français du pétrole*, Dec. 1963, 18, 1-16.

4 Takhar S. (1995) Prediction of asphaltene aeposition during production - Model description and experimental details. *SPE* 30108, Eur. Formation Damage, The Hague, May 15-16.

5 Minssieux L., Bardon C., Rouet J. and Groffe P. (1995) Effects of asphaltenes deposition in production/treatment and prevention tests. *Symposium ISCOP'95*, Rio, Nov. 26-29, Proc. 129-134.

6 Galopini M. and Tambini M. (1994) Asphaltene deposition monitoring and removal treatments: an experience in ultra deep wells. *SPE* 27622, 1994 European Prod. Operations Conf.

7 Brennand M. and Silva M.I.O. (1995) Removal of asphaltene deposition through xylene Injections. *Symposium ISCOP'95*, Rio, Nov. 26-29, Proc. 207-215.

8 Peden J.M. and Husain M.I. (1985) Visual investigation of multiphase flow and phase interactions within porous media. *SPE* 14307, Las Vegas, Sept. 22-25.

9 Chang C.L. and Fogler H.S. (1993) Asphaltene stabilization in alkyl solvents using oil-soluble amphiphiles. *SPE* 25185, Symp. Oilfield Chem., New Orleans, March 2-5.

10 Piro G., Canonico L.B., Galbariggi G., Berbero L. and Carniani C. (1995) Experimental study on asphaltene adsorption onto formation rock: an approach to asphaltene formation damage prevention. *SPE* 30109, Eur. Formation Damage Conf., The Hague, May 15-16.

11 de Pedrosa T.M. *et al. (*1994) Impact of asphaltene presence in some rock properties. *III Latin Am./Caribbean Petr. Eng. Conf.*, Buenos Aires, April 27-29.

12 Mitchell D.L. and Speight J.G. (1973) The solubility of asphaltenes in hydrocarbons solvents. *Fuel*, 52, 149-152.

13 Trabelsi K., Espitalié J. and Huc A.Y. (1994) Characterisation of extra oils and tar deposits by modified pyrolysis methods. *Symposium on Heavy Oil Technologies in a Wider Europe*, Berlin, June, 7-8.

14 Burke N.E. *et al.* (1990) Measurement and modeling of asphaltene precipitation. *JPT*, Nov. 1990, 1440-1446.

15 Gonzales G. and Travalloni-Louvisse A.M. (1993) Adsorption of asphaltenes and its effect on oil production. *SPE* Prod. Facil., May 1993, 91-96.

16 Collins S.H. and Melrose J.C. (1983) Adsorption of asphaltenes and water on reservoir rock minerals. *SPE* 11800, Symp. Oil and Geo. Chem., Denver, June 1-3.

17 Sheu E.Y. and Mullins O.C. (1995) *Asphaltenes Fundamentals and Applications*, Plenum Press ed., New York, 145-147.

18 Roque C., Chauveteau G. *et al.* (1995) Mechanisms of formation damage by retention of particles suspended in injection water. *SPE* 30110, European Formation Damage Conf., La Hague, May 15-16.

19 Gruesbeck C. and Collins R.E. (1982) Entrainment and deposition of fine particles in porous media. *Soc. Petr. Eng. J.*, Dec. 1982, 847-856.

20 Wojtanowicz A.K. *et al. (*1987) Study on the effect of pore blocking mechanisms on formation damage. *SPE* 16233, Prod. Operations Symposium, Oklahoma City, March 8-10.

21 Nabzar L., Chauveteau G. and Roque C. (1996) A new model for formation damage by particle retention. *SPE* 31119, International Symposium on Formation Damage Control, Lafayette, Louisiana, USA, February 14-15.

22 Chauveteau G., Nabzar L. and Coste J.P. (1998) Physics and modeling of permeability damage induced by particle deposition. *SPE* 39463, International Symposium on Formation Damage Control, Lafayette, Louisiana, USA, February 18-19.

23 Chauveteau G., Nabzar L., El Attar Y. and Jacquin C. (1996) Pore structure and hydrodynamic in sandstones. *SCA* 9607, International Symposium of Society of Core Analysts, Montpellier, France, September 8-10.

24 Nabzar L. and Chauveteau G. (1997) Permeability damage by deposition of colloidal particles. *SPE* 38160, European Formation Damage Conference, The Hague, The Netherlands, June 2-3.

25 Priveman V., Frish H.L., Ryde N. and Matijevic E. (1991) *J. Chem. Soc.*, Faraday Trans., 87, 1371.

26 Nabzar L., Coste J.P. and Chauveteau G. (1997) Water quality and well injectivity. *Paper* 044, *9th European Symposium on Improved Oil Recovery*, The Hague, The Netherlands, October 20-22.

27 Ravey J.C. and Espinat D. (1990) Macrostructure of petroleum asphaltenes by small angle neutron scattering. *Progr. Colloid Polym. Sci.*, 81, 127-130.

Final manuscript received in March 1998